Thin polymer films on chemically patterned, corrugated substrates

2005 J. Phys.: Condens. Matter 17 S389

(http://iopscience.iop.org/0953-8984/17/9/007)

INSTITUTE OF PHYSICS PUBLISHING JOURNAL OF PHYSICS: CONDENSED MATTER

J. Phys.: Condens. Matter **17** (2005) S389–S402 doi:10.1088/0953-8984/17/9/007

Thin polymer films on chemically patterned, corrugated substrates

Mark Geoghegan[1,3], Chun Wang[2], Nicolaus Rehse[2], Robert Magerle[2] and Georg Krausch[2,3]

[1] Department of Physics and Astronomy, University of Sheffield, Hicks Building, Hounsfield Road, Sheffield S3 7RH, UK
[2] Lehrstuhl für Physikalische Chemie II and Bayreuther Zentrum für Kolloide und Grenzflächen (BZKG), Universität Bayreuth, D-95440 Bayreuth, Germany

E-mail: mark.geoghegan@sheffield.ac.uk and georg.krausch@uni-bayreuth.de

Received 24 November 2004
Published 18 February 2005
Online at stacks.iop.org/JPhysCM/17/S389

Abstract

We study the effect of a chemical pattern on the wetting and dewetting behaviour of thin polystyrene (PS) films on regularly corrugated silicon substrates. Our results reveal that the film preparation, annealing method, and confinement play a critical role in the final film structure. On evaporating gold on both sides of the facets (such that it covered the crests of the facets, and not the troughs), we observed dewetting, which proceeded to the gold, demonstrating an enthalpic effect contrary to the outcome previously observed when gold was only evaporated on one side of the facet. We also coated the substrate with octadecyltrichlorosilane (OTS); this led to a gold and OTS striped structure. PS films several nanometres thick dewet such substrates, with a preferential direction for dewetting in the direction of the stripes forming droplets of a considerably larger size than the stripes.

1. Introduction

The control and growth of surface structures has a wide variety of applications such as in microelectronics, catalysis, and lithography. One particularly useful aspect of structured substrates is the ability to chemically pattern a substrate in order to achieve preferential adsorption of one component [1–5]. Patterned model substrates have been prepared following different routes. In order to produce micron-scale surface energy patterns, different types of lithography have been applied [1, 6, 7]. A general tendency is that the overall lateral dimensions of the patterned area created using such techniques decrease with decreasing pattern size. Alternatively, self-assembly processes can be utilized with the potential to create patterns of nanoscopic characteristic lengths over macroscopically large areas [4, 8, 9].

[3] Authors to whom any correspondence should be addressed.

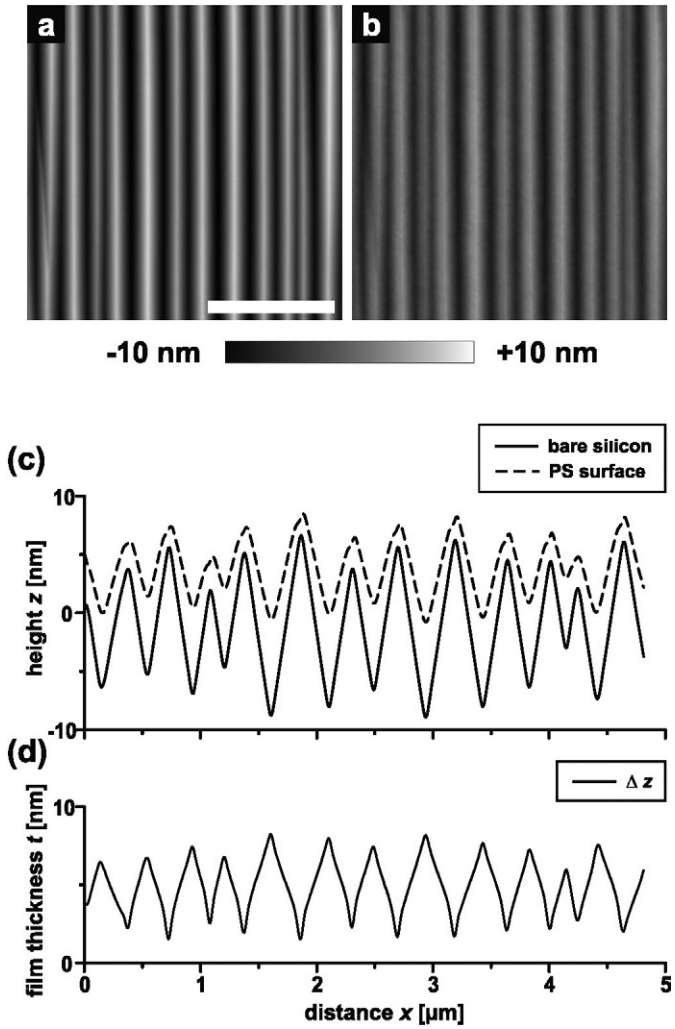

Figure 1. (a) An SFM scan of a faceted silicon substrate with a mean width of ∼400 nm. (b) An SFM scan of the same spot after coating with a PS layer ($t_{\mathrm{av}} = 5$ nm, $M_{\mathrm{w}} = 100$ kDa). In (c) we show average line scans (i.e. the height averaged along the direction of the facets) for both of these SFM images. This clearly shows that in the troughs of the structure, the PS film is thicker than it is at the peaks. (d) The difference in height between the silicon and PS surfaces is calculated considering the separate measurement of t_{av}. The peaks in the height difference calculation (d) correspond to the troughs in the line scans shown in (c). The scale bar corresponds to 2 μm.

The stability of polymer films on chemically patterned and/or topographically rough surfaces is of great current interest [10–13]. In our previous work, we considered the stability of thin polystyrene (PS) films on silicon substrates with a sawtooth or corrugated structure [14]. Such substrates are readily produced by ultrahigh vacuum annealing of suitably miscut silicon single crystals [15–17]. A surface faceting transition causes the surface to develop nanoscopic corrugations of well-defined mean spacing. The corrugations follow the respective crystal orientation and therefore are aligned over macroscopic distances (figure 1(a)). When a thin polymer film of average thickness t_{av} is spin cast onto such substrates from solution, the film

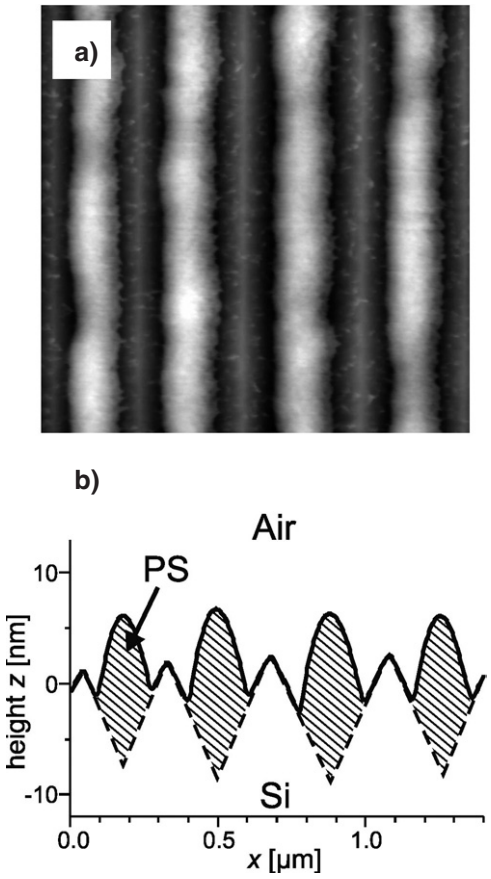

Figure 2. Top: an SFM TappingMode^{TM} topography image (1.5 × 1.5 μm^2) of a thin PS film (M_w = 100 kDa, t_{av} = 5 nm) on a corrugated silicon substrate after annealing at 150 °C for 3 h. The film has broken into linear channels following the grooves of the substrate. Bottom: an average line scan along the horizontal taken from the image (b). The solid curve is the experimental result. The dashed line depicts the position of the substrate surface. (Reproduced with permission from [14], ©2001 EDP Sciences.)

surface follows the corrugations. To illustrate the effect of coating the substrate with a polymer film, in figures 1(a) and (b) we show two TappingMode^{TM} scanning force microscopy (SFM) images of a corrugated silicon substrate taken at the same spot before and after coating with a thin PS layer. The corrugated structure clearly remains after coating with the PS layer but the troughs in the structure are not as deep as before coating. This is due to surface tension minimizing curvature in the film. As a result the film thickness varies laterally (i.e. is thicker in the troughs and thinner on the peaks (see figures 1(c) and (d))).

It was found that PS films become unstable upon heating on such nanoscopically corrugated substrates and form nanochannels filling the grooves of the pattern (figure 2) [14]. This instability occurred only when the film thickness at the crests of the corrugation became thinner than about half their bulk radius of gyration of the polymer chains, suggesting that chain deformation plays a role in determining the film stability. In our previous study [14], as well as in an earlier work [4], every other facet of the substrate was coated with metal (gold), creating an additional chemical pattern. Here enthalpic effects are also important and the affinity of the

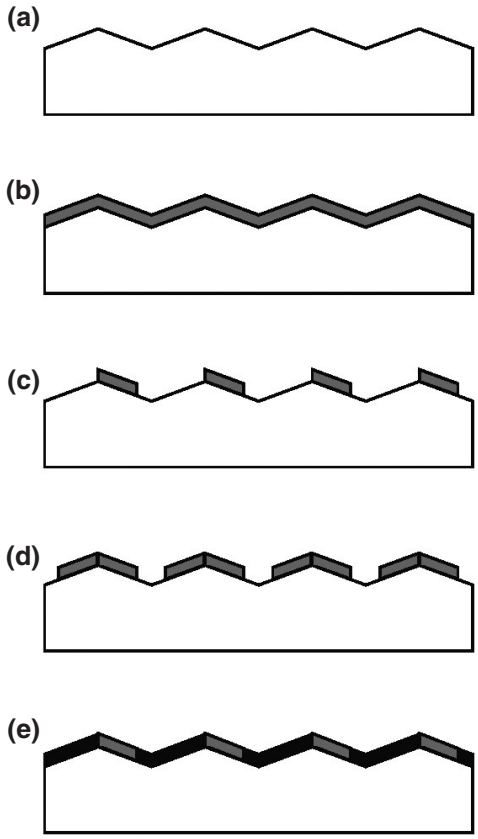

Figure 3. Schematic drawings of the substrates used in this paper. For an explanation, see the text.

PS for the gold can be observed because the final dewetted structure is asymmetric, with the polymer partially coating the gold.

In the present paper we report in more detail on the stability of thin polymer films on both topographically and chemically patterned substrates, including experiments aimed at elucidating the time dependence of the dewetting process. In addition, we vary the nature of the chemical pattern on the corrugated substrates and study corrugated silicon oxide surfaces, corrugated gold surfaces, alternating lines of gold and silicon oxide, and alternating lines of gold and octadecyltrichlorosilane (OTS). In figure 3 we show schematically the substrates from which the dewetting is studied. We commence with the kinetics of dewetting from silicon oxide-coated silicon (figure 3(a)), where we introduce the idea that sample preparation is likely to have some effect in the dewetting process. This discussion is followed by a demonstration that gold-covered corrugated substrates (figure 3(b)) provide a stable surface for PS. Having discussed the effect of gold and silicon oxide surfaces, we show how a chemical pattern of gold and silicon oxide (figures 3(c) and (d)) affects the dewetting; PS dewets the corrugated substrates with a rather asymmetric structure when one facet is covered with gold. If both facets are covered with gold (figure 3(d)), then the enthalpic attraction of PS for gold is observed via a preferential wetting of gold by the PS. Finally, we provide data demonstrating the effect of an alternating corrugated structure of gold and OTS (figure 3(e)). Although the

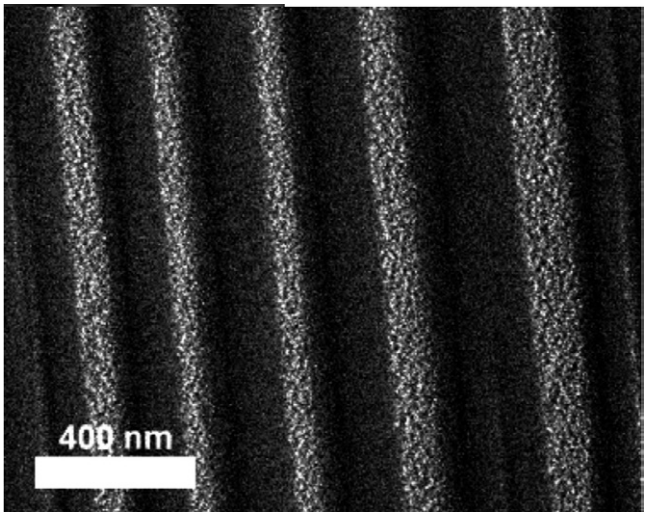

Figure 4. An FE-SEM image of a faceted silicon substrate with gold covering the tops of the grooves. In this case, the gold was only evaporated onto one side of the facets.

gold surface is one that the PS would generally wet, the driving force for dewetting of the OTS creates a dramatic dewetting structure for thicker polystyrene films, which can be attributed to anisotropic spinodal dewetting [18].

2. Experimental details

The details of the preparation of the corrugated substrates have been presented elsewhere [14–17], and so a brief review of the method will suffice here. We used polished silicon wafers ($5 \times 12 \times 0.5$ mm^3) with the surface normal pointing $3^\circ \pm 0.5^\circ$ off the $\langle 113 \rangle$ crystal axis towards the $\langle 001 \rangle$ axis (Crystec, Berlin). In order to enable the use of resistive heating, we chose arsenic doped (n-type) silicon. The samples were annealed at temperatures up to 1250 °C under ultrahigh vacuum conditions (10^{-9} mbar) to remove the native oxide layer. The sample was then cooled to temperatures around 800 °C and kept there for various times (typically ∼1 h) to allow surface facets to grow [15–17]. The wafers were quenched to room temperature and were then exposed to ambient atmosphere. A thin (∼2 nm) layer of native silicon oxide is formed during this last step of the process. Oxide formation, however, leaves the corrugated pattern intact, as can be seen in figure 1(a).

Glancing angle (∼2°) evaporation of a metal onto the corrugated silicon substrates is an effective means of providing a chemical pattern on the substrate. Gold is a particularly good choice of metal for this patterning because thiol chemistry can then be used to further tailor the surface properties. Best results were obtained by performing this evaporation in a two-stage process with a chromium adhesion layer (of thickness ∼2 nm) deposited first, followed by gold (of thickness ∼5 nm). This evaporation scheme leads to an asymmetric pattern with only every other facet coated with gold. In figure 4, we show a field emission scanning electron micrograph of a surface prepared in this way. The use of a field emission gun ensures a coherent electron beam, which enables chemical contrast in the electron micrographs. In order to reach a symmetric metal coating of the crests, some of the substrates were rotated by 180° about the surface normal and the evaporation process was repeated. In this case, SiO_x remained

exposed only in the troughs of the corrugated structure. Some of the substrates prepared in this way were further modified by silanation of the uncovered SiO_x parts within the troughs using octadecyltrichlorosilane (OTS) [19]. This procedure leaves a chemical pattern with larger contrast of the surface energies of the different lines. Finally, in order to create corrugated substrates without chemical heterogeneity, but with a different surface chemistry, some of the corrugated substrates were completely coated with gold by evaporating the two metals onto the corrugated silicon substrate with an angle of 90° between the surface and the metal beam.

Thin polystyrene films were spin coated onto the substrates both with and without additional surface modification.

All samples were imaged with TappingMode™ SFM after each preparation step. In some experiments, it was necessary to image the same region as before. Such regions were easily located by using a scratch or other defect in the film, which helped identify the region of interest. No images were taken so close to the scratch that it affected the film structure.

In the following, we use the notation of our previous paper [14] and quote the average film thickness, t_{av}, which is the thickness of the film when the same solution is spin coated onto a clean, flat, silicon wafer.

3. Results and discussion

3.1. Corrugated, chemically homogeneous substrates: SiO_x

The initial motivation for studying the kinetics of dewetting was to elucidate the mechanism for the formation of the final structure. To facilitate our measurements we slowed the kinetics by lowering the annealing temperature from 150 and 180 °C [14] to 120 °C. All measurements were performed *ex situ*, with the sample being reheated after each measurement. We chose PS films with $M_w = 100$ kDa and $t_{av} = 5$ nm, because these would be expected to form nanochannels since their formation occurs when the thickness of the film at the crests of the peaks, t_{peak}, is less than about half the polymer radius of gyration, R_g ($t_{peak} \approx 2$ nm, $R_g = 8$ nm). Indeed, after 3 min of annealing at 120 °C, holes are observed at the crests of the corrugation (figure 5(b)). However, after the initial formation of holes in the polymer film, no further changes are observed on extended annealing (figures 5(c)–(e)). Even subsequent annealing at increased temperatures of 150 °C (figures 5(f) and (g)) and 180 °C (figure 5(h)) left the structure unchanged.

The stability of the polymer films after annealing for a short while at a low temperature is in marked contrast to the complete dewetting of the films at high temperature. This raises the question of why the dewetting stops after this first annealing step despite holes having being nucleated in the film. One can suppose that the initial (spontaneous) formation of the holes occurs in both cases. The holes formed on the peaks of the sawtooth structure may well have been due to a process such as thermal nucleation, and a confinement-related effect could have driven the dewetting to its conclusion in the high temperature annealing case. (We doubt that a spinodal process is responsible for the dewetting because this would have selected and amplified a particular length scale for the dewetting and there is no evidence for this in our data, and nor is it easy to see why a spinodal process would be responsible for dewetting in our films.) In the case of films removed from the oven after heating, the driving force for dewetting is clearly removed. It is possible therefore that the polymer chains have relaxed to a more stable conformation, whereby confinement has no effect on the dewetting.

We suggest that, besides confinement, there is a second effect, which is important in such films, and was briefly discussed in our previous paper [14]. The suggestion is that during spin coating, the film vitrifies before all of the solvent has evaporated, which may lead to some

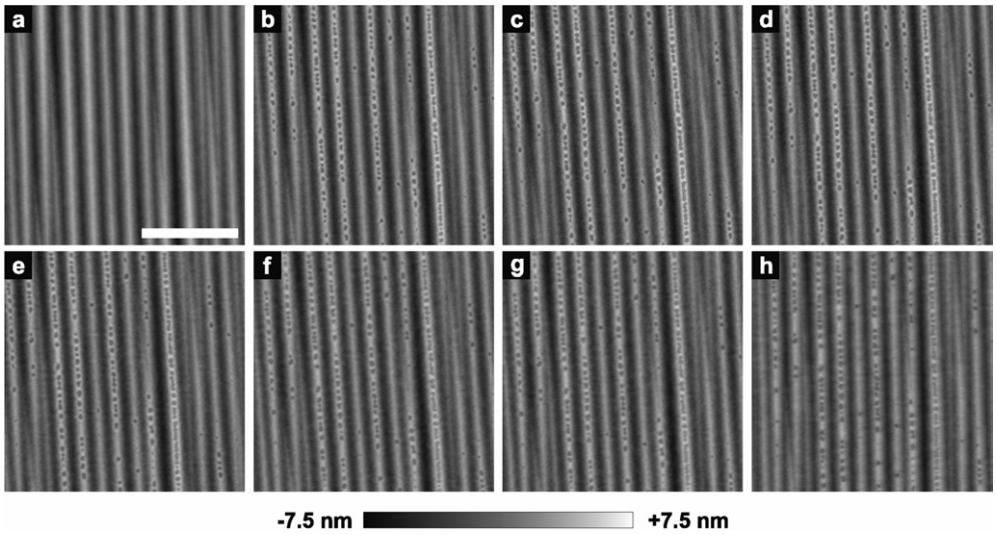

Figure 5. SFM scans of a PS film ($t_{av} = 5$ nm, $M_w = 100$ kDa) coated onto a faceted silicon substrate. The image in (a) corresponds to the unannealed sample; (b) is the same region after annealing for 3 min at 120 °C. The annealing was then incremented by (c) 3 min at 120 °C, (d) 15 min at 120 °C, (e) 60 min at 120 °C, (f) 15 min at 150 °C, (g) 60 min at 180 °C, and (h) 14 h at 180 °C. All annealing was performed under an N_2 atmosphere except that of (h), which was performed in air, which probably left this sample oxidized. The scale bar corresponds to 2 μm.

internal stress in the film. In this case one could suppose that the holes formed at the start of the dewetting process were nucleated by polymer chain distortions frozen in during spin coating. Such an explanation is also consistent with the observed effect; the dewetting would be expected to start at the thinnest points on the film (the peaks of the corrugations).

Another possible contribution to this 'second effect' that we should also mention is the thermal expansion on heating a film of ∼4 nm thickness up to 120 °C. Previous measurements on polystyrene films on etched silicon indicate a ∼10% increase in film thickness [20]. Any chain distortions creating an internal stress would then be able to relax after the heat treatment was terminated. After relaxation there is no driving force for further hole growth. Other preparation effects, for example, involving residual solvent, are unlikely because they would not explain the molecular weight dependence of the film stability [14].

Unfortunately, it is difficult to see how such preparation effects may be experimentally tested. Spin coating is a highly non-equilibrium process that is unlikely to leave polymer chains in thin films with a Gaussian (random coil) conformation. As a result, the need of a polymer chain on the peaks of the structure to lower its free energy by having a Gaussian conformation causes it to dewet to the troughs of the corrugations. The removal of what we refer to as 'internal stress' does not mean that the chain need have a truly random conformation, which would require thicker films; it may obtain a stable conformation of the type described by Silberberg [21], whereby a chain can be conformationally stable through reflections in its random walk conformation whenever this conformation passes across the interface.

3.2. Corrugated, chemically homogeneous substrates: gold

To distinguish the different contributions to the observed dewetting, we have studied the stability of a $t_{av} = 5$ nm thick PS film ($M_w = 100$ kDa) on a corrugated substrate covered

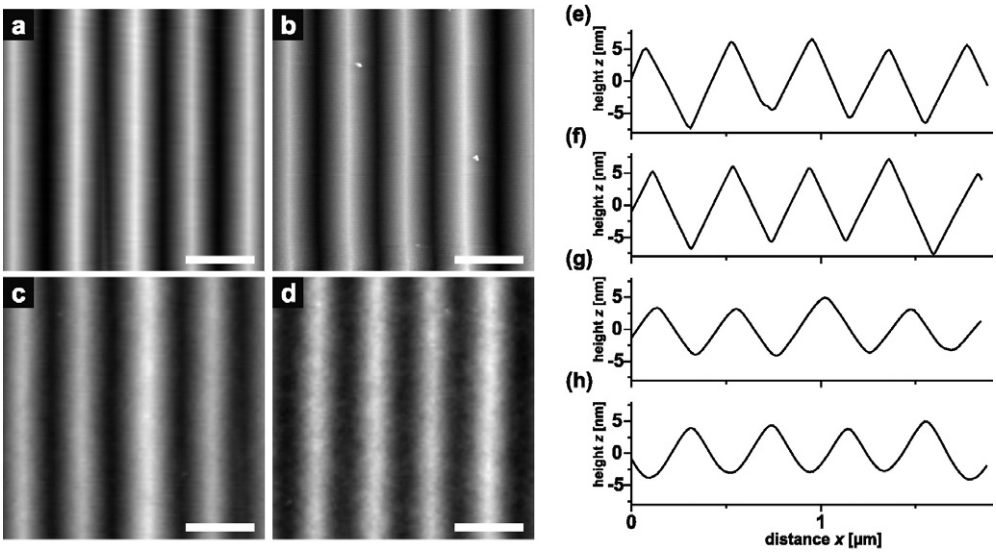

Figure 6. SFM scans and average line scans for a corrugated silicon substrate, ((a), (e)) as prepared, ((b), (f)) after completely covering the substrate with evaporated chrome and then gold, ((c), (g)) after coating with a PS film, and ((d), (h)) after annealing the film for 10 min at 180 °C under N_2. The original film has an average thickness $t_{av} = 5$ nm, and the polymer has $M_w = 100$ kDa. The scale bar corresponds to 500 nm.

entirely with gold (figure 6). In this case the film was found to remain stable even after annealing at 180 °C for 10 min under N_2, which suggests that the attractive interaction between PS and gold dominates over all other contributions.

3.3. Corrugated and chemically patterned substrates: gold/SiO_x

In our previous paper [14] we presented our first experimental results for polystyrene dewetting a substrate consisting of gold and SiO_x stripes (similar to the work reported by Rockford *et al* [4]). Our results were different from those for substrates with no gold present; the shape of the dewetted structure was asymmetric, with the polymer preferentially adsorbing onto the gold. Detailed inspection of the respective samples reveals that the thinnest parts of the films, which are located on top of the gold-covered peaks, also dewetted. This can be seen from the FE-SEM image shown in figure 7, which shows a clear material contrast between SiO_x, gold, and PS. This finding again indicates that aside from the enthalpic driving force, a second origin of the film instability exists, which is of entropic nature and is related to the confinement of the chains.

To study the kinetics of dewetting we performed an experiment similar to the one shown above on the chemically homogeneous substrates. In this case, only one side of the crests was coated with metal. As can be seen in figure 8, the dewetting behaviour on such chemically patterned substrates appears to be somewhat different from that on the chemically homogeneous ones. Again, holes are formed on top of the crests initially. However, on extended annealing at elevated temperatures the dewetting could be driven to completion (figure 8). Finally, the PS film has broken into nanochannels, which are located asymmetrically on the gold-covered sides of the crests. As indicated above (figure 7), the gold-coated peaks of the crests are dewetted as well.

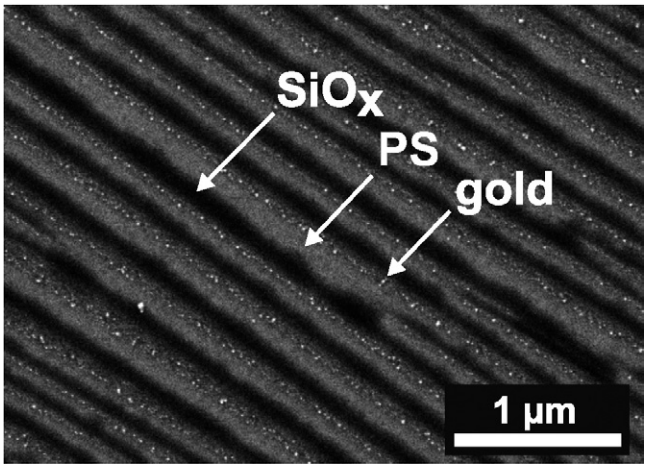

Figure 7. An FE-SEM image of a PS film (100 kDa, $t_{av} = 5$ nm) coated onto a substrate alternating with SiO_x and gold (this image is from the same sample as in figure 8(h)). The chemical contrast provided by FE-SEM clearly indicates that the PS does not completely wet the gold-covered peaks of the substrate.

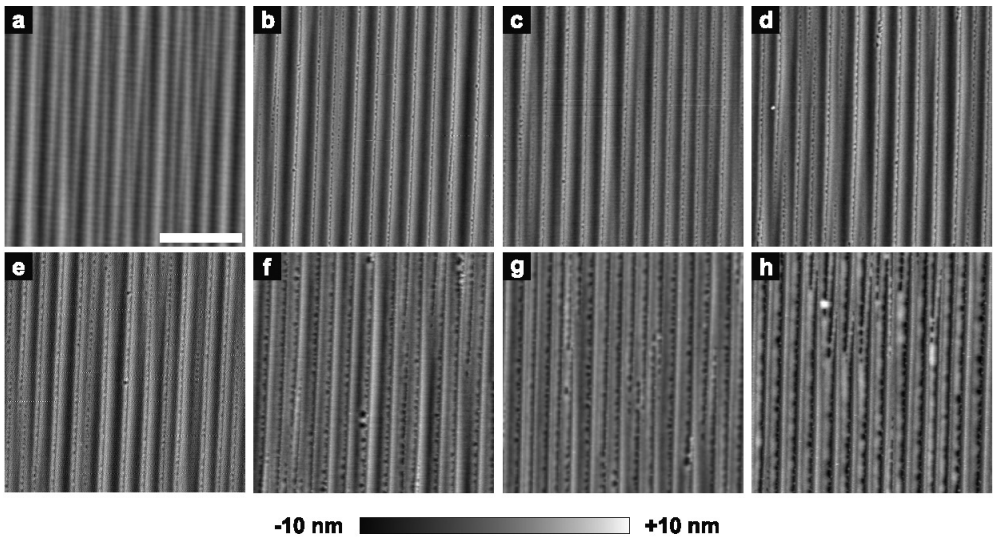

Figure 8. SFM images of a PS film ($t_{av} = 5$ nm, $M_w = 100$ kDa) coated onto a substrate alternating with SiO_x (troughs of the corrugations) and gold (right-hand sides of the peaks). The image in (a) corresponds to the unannealed sample; (b) is the same region after annealing for 2 min at 105 °C. The annealing was then incremented by (c) 3 min at 105 °C, (d) 30 min at 105 °C, (e) 1.5 min at 120 °C, (f) 5 h at 120 °C, (g) 60 min at 180 °C, and (h) 7 h at 180 °C. All annealing was performed under an N_2 atmosphere. In contrast to the data shown in figure 5, nanochannels are formed. The scale bar corresponds to 2 μm.

This corroborates the assumption that residual internal stress is initiating the hole formation on top of the crests because the roughness of the gold stripes further facilitates the dewetting of the crests.

We now consider how thin PS films wet a corrugated substrate after the gold has been evaporated on *both* sides of the facets, leaving an SiO_x surface only within the troughs. After

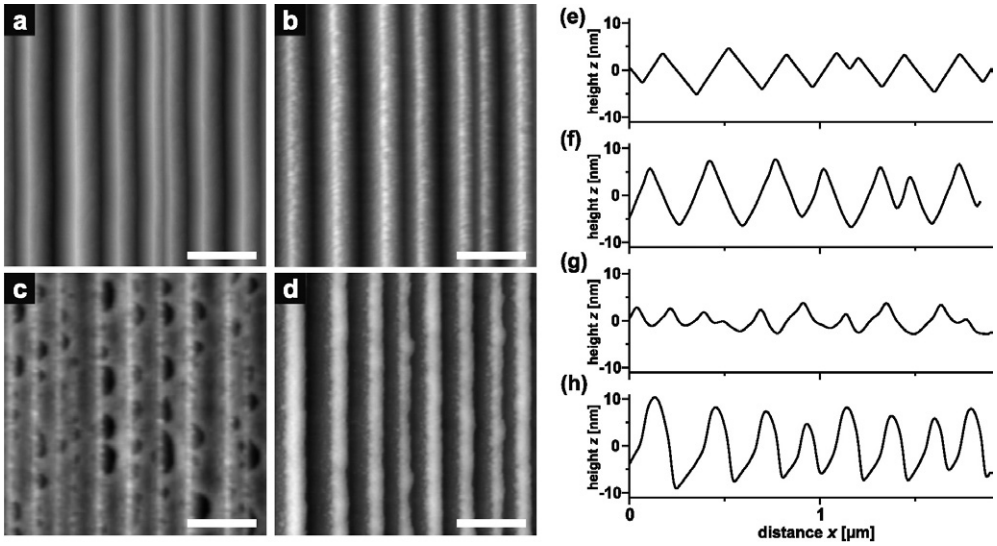

Figure 9. SFM scans and average line scans for a corrugated silicon substrate, ((a), (e)) as prepared, ((b), (f)) after completely covering the substrate with evaporated chrome and then gold on both sides (the right-hand side of the substrate was exposed to the vapour first), ((c), (g)) after coating with a PS film ($M_w = 5$ kDa, $t_{av} = 2$ nm), and ((d), (h)) after annealing the film for 10 min at 180 °C under N_2. Note that the PS does not efficiently wet the substrate after spin coating but does manage to wet the gold very efficiently after annealing. The scale bar corresponds to 500 nm.

evaporation of chromium, the sample was rotated by 180° and more chromium was evaporated on the other side of the facets. The process was then repeated for gold. This means that gold covers both sides of the peaks, as can be seen from the AFM image and the averaged line scans shown in figure 9(b). For these experiments we used $M_w = 5$ kDa in a $t_{av} = 2$ nm layer, which would be expected to readily dewet a faceted substrate with only a native oxide layer present on the surface. The film was spin coated onto the substrate and annealed in a N_2 atmosphere. The spin-coated film dewets the substrate in an anisotropic fashion, but after annealing the polystyrene prefers to wet the gold. Again nanochannels are formed, but this time on the crests of the structure. A large (5 μm) scan of the subsequent morphology is shown in figure 10. In this experiment it is clear that the enthalpic attraction from the gold outweighs an entropic confinement-induced dewetting. A probable reason for this structure is the fact that the polymer did not completely wet the silicon after spin coating. This means that the formation of nanochannels in the SiO_x troughs would be highly unlikely since it would entail the formation of a high energy SiO_x–PS interface.

3.4. Corrugated and chemically patterned substrates: gold/OTS

We can further modify the wetting conditions of the substrates discussed above by the inclusion of an OTS layer between the gold stripes. To this end, a silanation was performed following standard procedures [19] after the gold was deposited. Otherwise the sample preparation is the same, with 20 and 60 nm films of polystyrene (with $M_w = 19$ and 100 kDa respectively) spin coated onto the substrate. We worked with relatively thick films (20 and 60 nm) because ultrathin films were already found to be unstable on these substrates during spin coating and annealing had little effect on the subsequent morphology. This finding is known for silicon surfaces homogeneously coated with methyl-terminated self-assembled monolayers. In the

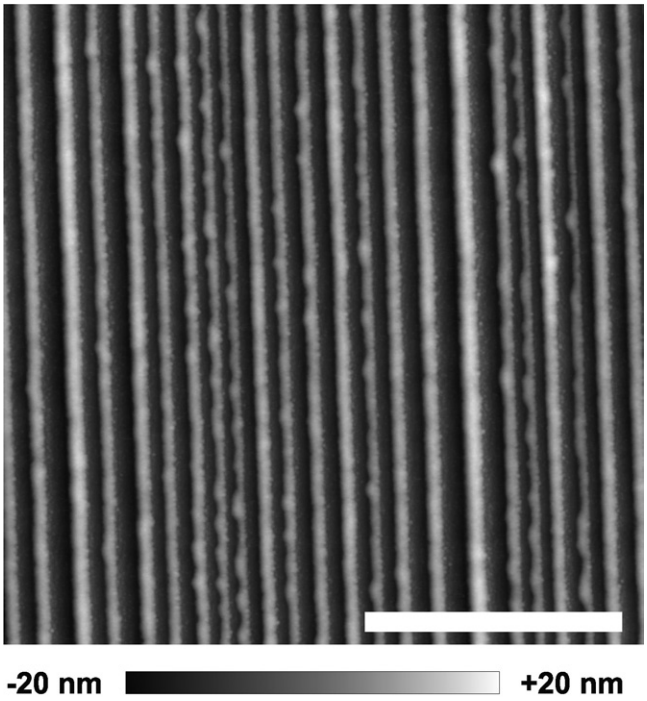

Figure 10. An SFM scan of a PS layer ($M_w = 5$ kDa, $t_{av} = 2$ nm) after annealing for 10 min at 180 °C under N_2. Here the PS has formed nanochannels, which preferentially wet the gold. This is the same sample as that shown in figure 9(d). The scale bar corresponds to 2 μm.

case of the patterned surface, the laterally averaged surface energy will still be considerably lower than those on SiO_x and on gold.

The optical micrograph in figure 11 shows the resulting morphology of the thinner of the two films after annealing. We see that droplets have formed with a size that is considerably larger than the characteristic spacing of the patterned substrate. On closer inspection we see that the resulting dewetting pattern is anisotropic. The droplet pattern is aligned along the direction of the stripes. This effect can be clearly seen in the fast Fourier transform (FFT) of the optical micrograph shown in the inset to figure 11. The observation of a coupling between the direction of the corrugations and the dewetting pattern is even more striking given the different length scales of the droplets and the stripes. We note that this behaviour is a good example of anisotropic spinodal dewetting observed recently in bilayers of polymethylmethacrylate (PMMA) on PS [18]. In this work, the dewetting proceeded because PMMA is intrinsically unstable on PS. An anisotropic pattern was imposed by rubbing the underlying glass substrate with a lens cleaning tissue prior to PMMA deposition. This was all that was necessary to impose a direction on the dewetting. The PMMA selected its own length scale during dewetting [22, 23]. The same seems to be happening in our system. The PS is intrinsically unstable on the substrate because the driving force for dewetting on OTS is very much stronger than the stabilizing attraction to the gold. On dewetting, a preferential direction is imposed by the substrate structure in a similar way to how a surface imposes a direction on phase separation in polymer blend films [24]. It is interesting to note that the fast Fourier transform of the optical micrograph does not reflect any dominant length scale, which would be expected from a spinodal dewetting mechanism. The dewetting may well take place in a two-stage

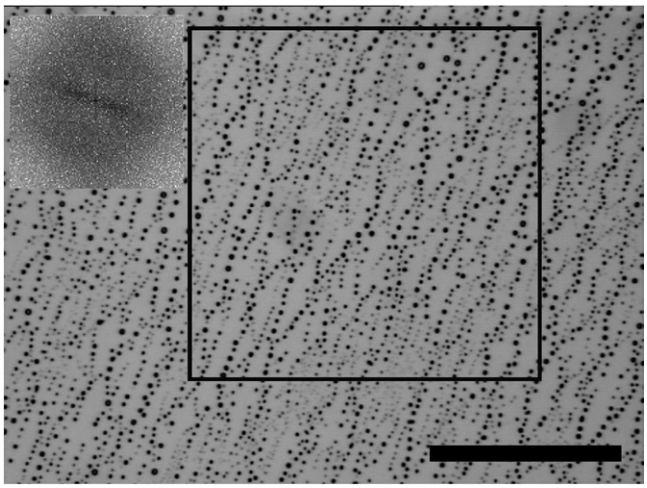

Figure 11. An optical microscopy image of a 20 nm film ($M_w = 19$ kDa) of PS spin coated onto a corrugated silicon substrate coated with alternating gold and OTS stripes along the facets. The film was annealed for 155 min at 150 °C. The inset shows a fast Fourier transform of the square section, indicating that a preferred orientation exists. The scale bar is 50 μm.

mechanism: first spinodal dewetting forces the direction of the phase separation along the direction of the facets, and secondly the lines break up via a Rayleigh capillary instability. At such a late stage as that observed here, the droplets cannot easily be identified as having been caused by spinodal dewetting.

For the 60 nm film, the PS layer is too thick for spinodal dewetting to drive the phase separation, either because the dewetting proceeds too slowly, or because the effect of gravity stabilizes the film. In this case, the only dewetting process is nucleation and growth. A nucleated hole is shown in figure 12. However, although we do not see the large scale phase separation of the 20 nm film, there is still a dominant direction observed in the hole due to pinning of the dewetting rim by the structure of the substrate.

4. Conclusions

We have followed up our earlier work [14] on the influence of the molecular weight on the stability of PS films on a corrugated silicon substrate by exploring the kinetic behaviour of dewetting and varying the chemical nature of the substrate surface. PS films dewet a substrate coated with gold at the top of one side of each facet via the formation of holes, which grow, and the film eventually breaks up, forming nanochannels. However, on a pure SiO_x sawtooth surface, the PS film remains stable, after the initial formation of holes at the peaks of the corrugations. We suggest that a preparation effect, a relaxation of internal stress in the as-cast films, is responsible for the behaviour. The reason that the two kinetics are different is at present unclear.

We considered the equilibrium structure of PS dewetting from substrates in which the peaks of the facets were symmetrically coated with gold. Here nanochannels are formed and they preferentially adsorb to one side of the facets, but they do coat the crests of the facets. This is in contrast to the case for one-sided evaporation, where the peaks were dewetted. In this case the enthalpic effect appears to be strong enough to outweigh any entropic confinement-induced dewetting.

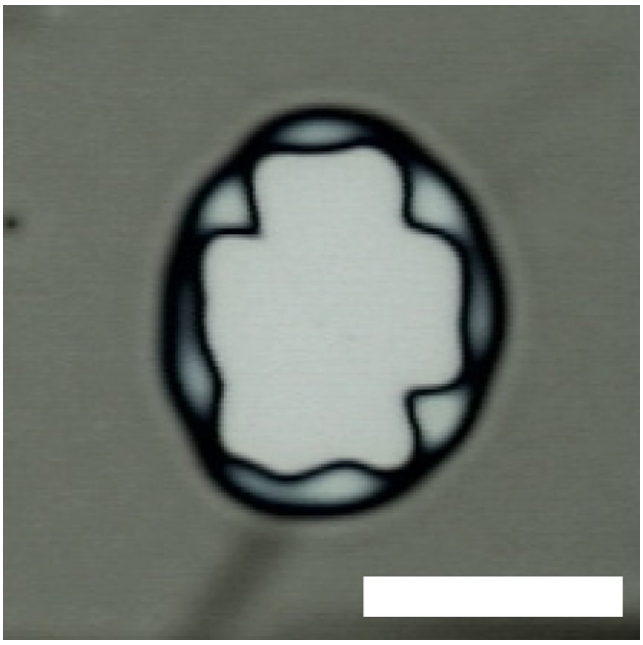

Figure 12. An optical microscopy image of a hole in a 60 nm film ($M_w = 100$ kDa) of PS deposited on a corrugated silicon substrate coated with alternating gold and OTS stripes along the facets. The film was annealed for 65 min at 180 °C. The scale bar corresponds to 20 μm. The direction of the corrugation is perpendicular to the scale bar.

(This figure is in colour only in the electronic version)

We have shown that with a chemical pattern for thicker films, anisotropic spinodal dewetting is observed. However, in the first work on this subject the length scale that imposed directionality is poorly defined [18]. In our case it is very well defined, and of the order of about 400 nm. This is considerably less than that of the droplet morphology formed on dewetting from OTS/gold striped substrates, which is of the order of several microns. This demonstrates that the hypothesis of Higgins and Jones, in which the dewetting selects its own length scale, independently of that imposed on it by the substrate, is correct. Thicker films only dewet by nucleation and growth, but even then the holes formed are not circular, but rather oval, with the longer axis parallel to the facet direction.

The ability to create structures with a dominant direction could have interesting properties of polarization. It could therefore be used as a method complementary to that proposed elsewhere for anti-reflection coatings [25]. However, before any applications can be considered using chemical patterning, it is crucial to understand both the effect of interactions with different materials and the influence of roughness and topology on the final structure.

Acknowledgments

This work was supported through the Deutsche Forschungsgemeinschaft (Schwerpunkt Benetzung und Strukturbildung an Grenzflächen, Contract No Kr1369/9). The skilful help of M Hund (in the preparation of the structured substrates) and C Abetz (SEM) is gratefully acknowledged. RM acknowledges support from the VolkswagenStiftung and MG acknowledges J de Silva for a useful discussion.

References

[1] Abbott N L, Folkers J P and Whitesides G M 1992 Manipulation of the wettability of surfaces on the 0.1- to 1-micrometer scale through micromachining and molecular self-assembly *Science* **257** 1380–2

[2] Herminghaus S, Fery A, Schlagowski S, Jacobs K, Seemann R, Gau H, Mönch W and Pompe T 2000 Liquid microstructures at solid interfaces *J. Phys.: Condens. Matter* **12** A57–74

[3] Liu Y, Rafailovich M H, Sokolov J, Schwarz S A, Zhong X, Eisenberg A, Kramer E J, Sauer B B and Satija S K 1994 Wetting behavior of homopolymer films on chemically similar block copolymer surfaces *Phys. Rev. Lett.* **73** 440–3

[4] Rockford L, Liu Y, Mansky P, Russell T P, Yoon M and Mochrie S G J 1999 Polymers on nanoperiodic heterogeneous surfaces *Phys. Rev. Lett.* **82** 2602–5

[5] Rockford L, Mochrie S G J and Russell T P 2001 Propagation of nanopatterned substrate templated ordering of block copolymers in thick films *Macromolecules* **34** 1487–92

[6] Böltau M, Walheim S, Mlynek J, Krausch G and Steiner U 1998 Surface-induced structure formation of polymer blends on patterned substrates *Nature* **391** 877–9

[7] Xia Y, Zhao X-M and Whitesides G M 1996 Pattern transfer: self-assembled monolayers as ultrathin resists *Microelectron. Eng.* **32** 255–68

[8] Fasolka M J, Harris D J, Mayes A M, Yoon M and Mochrie S G J 1997 Observed substrate topography-mediated lateral patterning of diblock copolymer films *Phys. Rev. Lett.* **79** 3018–21

[9] Fukunaga K, Elbs H and Krausch G 2000 Thin film phase separation on a nanoscopically patterned substrate *Langmuir* **16** 3474–7

[10] de Gennes P G 1985 Wetting: statics and dynamics *Rev. Mod. Phys.* **57** 827–63

[11] Findenegg G H and Herminghaus S 1997 Wetting: statics and dynamics *Curr. Opin. Colloid Interface Sci.* **2** 301–7

[12] Geoghegan M and Krausch G 2003 Wetting at polymer surfaces and interfaces *Prog. Polym. Sci.* **28** 261–302

[13] Krausch G 1997 Dewetting at the interface between two immiscible polymers *J. Phys.: Condens. Matter* **9** 7741–52

[14] Rehse N, Wang C, Hund M, Geoghegan M, Magerle R and Krausch G 2001 Stability of thin polymer films on a corrugated substrate *Eur. Phys. J.* E **4** 69–76

[15] Song S and Mochrie S G J 1994 Tricriticality in the orientational phase diagram of stepped Si(113) surfaces *Phys. Rev. Lett.* **73** 995–8

[16] Song S and Mochrie S G J 1995 Attractive step–step interactions, tricriticality, and faceting in the orientational phase diagram of silicon surfaces between [113] and [114] *Phys. Rev.* B **51** 10068–84

[17] Song S, Mochrie S G J and Stephenson G B 1995 Faceting kinetics of stepped Si(113) surfaces: a time resolved x-ray scattering study *Phys. Rev. Lett.* **74** 5240–3

[18] Higgins A M and Jones R A L 2000 Anisotropic spinodal dewetting as a route to self-assembly of patterned surfaces *Nature* **404** 476–8

[19] Silberzan P, Léger L, Ausserré D and Benattar J J 1991 Silanation of silica surfaces. A new method of constructing pure or mixed monolayers *Langmuir* **7** 1647–51

[20] Keddie J L, Jones R A L and Cory R A 1994 Size-dependent depression of the glass transition temperature in polymer films *Europhys. Lett.* **27** 59–64

[21] Silberberg A 1982 Distribution of conformations and chain ends near the surface of a melt of linear flexible macromolecules *J. Colloid Interface Sci.* **90** 86–91

[22] Brochard Wyart F and Daillant J 1990 Drying of solids wetted by thin liquid films *Can. J. Phys.* **68** 1084–8

[23] Brochard Wyart F, Martin P and Redon C 1993 Liquid/liquid dewetting *Langmuir* **9** 3682–90

[24] Jones R A L, Norton L J, Kramer E J, Bates F S and Wiltzius P 1991 Surface-directed spinodal decomposition *Phys. Rev. Lett.* **66** 1326–9

[25] Walheim S, Schäffer E, Mlynek J and Steiner U 1999 Nanophase-separated polymer films as high-performance antireflection coatings *Nature* **283** 520–2